ACS SENSORS

pubs.acs.org/acssensors

Article

Biodegradable Smart Face Masks for Machine Learning-Assisted Chronic Respiratory Disease Diagnosis

Kaijun Zhang,[¶] Zhaoyang Li,[¶] Jianfeng Zhang, Dazhe Zhao, Yucong Pi, Yujun Shi, Renkun Wang, Peisheng Chen, Chaojie Li, Gangjin Chen, Iek Man Lei, and Junwen Zhong*

Cite This: *ACS Sens.* 2022, 7, 3135−3143

Read Online

ACCESS | Metrics & More | Article Recommendations | Supporting Information

ABSTRACT: Utilizing smart face masks to monitor and analyze respiratory signals is a convenient and effective method to give an early warning for chronic respiratory diseases. In this work, a smart face mask is proposed with an air-permeable and biodegradable self-powered breath sensor as the key component. This smart face mask is easily fabricated, comfortable to use, eco-friendly, and has sensitive and stable output performances in real wearable conditions. To verify the practicability, we use smart face masks to record respiratory signals of patients with chronic respiratory diseases when the patients do not have obvious symptoms. With the assistance of the machine learning algorithm of the bagged decision tree, the accuracy for distinguishing the healthy group and three groups of chronic respiratory diseases (asthma, bronchitis, and chronic obstructive pulmonary disease) is up to 95.5%. These results indicate that the strategy of this work is feasible and may promote the development of wearable health monitoring systems.

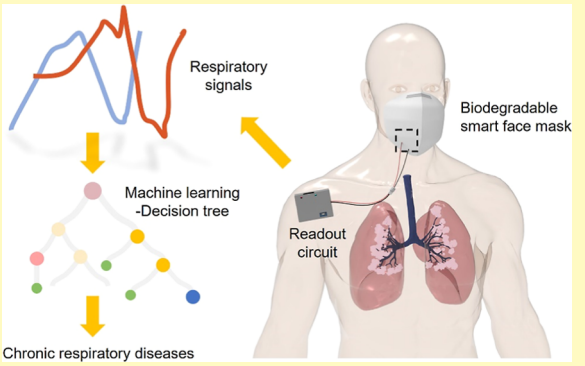

KEYWORDS: *smart face mask, self-powered sensors, biodegradable, machine learning, chronic respiratory disease diagnosis*

During the COVID-19 pandemic, people always needed to wear face masks to protect themselves and the quantity of face mask usage increased dramatically.[1−4] It has been reported that the average duration of wearing a face mask is 4−8 h per day for most people since the pandemic.[5] As a result, it is possible to construct a wearable and portable respiratory monitoring system with face masks as the basic platform to give an early warning to chronic respiratory diseases.[6,7] It should be noted that chronic respiratory diseases belong to common diseases.[8] For example, there are about 3.3 million people who suffer from the chronic obstructive pulmonary disease (COPD) all over the world.[9] In recent years, various sensors such as thermal ones,[10−12] humidity ones,[13−17] piezoresistive ones,[18,19] capacitive ones,[20,21] self-powered piezoelectric ones,[22,23] and self-powered electrostatic ones (including triboelectric[24−26] and electret[7,27,28] ones) have been assembled with face masks to measure the respiratory signals under normal or disordered conditions. The output performances of these sensors are good enough to capture the human respiratory signals and some of them are permeable. However, non-self-powered sensors need additional power sources, which will affect the weight, size, duration time, or complexity of the whole respiratory sensing system. On the other hand, most of the self-powered respiratory sensors are mainly based on environmentally unfriendly heavy-metal materials or nondegradable polymer materials, which will cause inevitable environmental concerns. It should be noted that real case studies are also lacking in previous works about smart face masks. Definitely, there are still some issues that limit the practicability of smart face masks.[6,11,29,30] A top-notch smart face mask should meet the following requirements: (1) the integrated sensors should have a fast response time, high sensitivity, and excellent output stability in real wearable conditions; (2) wearing comfort should be ensured, and it requires that a smart face mask should have good air permeability; (3) the duration for a smart face mask should be long, which means that self-powered sensors are preferred and the portable readout circuit must have low power consumption; (4) a smart face mask should be eco-friendly and have low cost because of the mass usage; thus, materials for constructing smart face masks should be mostly biodegradable and easily obtained; (5) real case studies should be performed to verify their practicality, the detected respiratory signals should be analyzed in an efficient way to accurately diagnose typical chronic respiratory diseases, and the corresponding machine learning algorithms need to be developed. In general, developing a smart face mask that can

Received: July 27, 2022
Accepted: September 23, 2022
Published: October 5, 2022

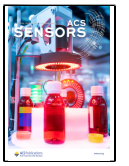

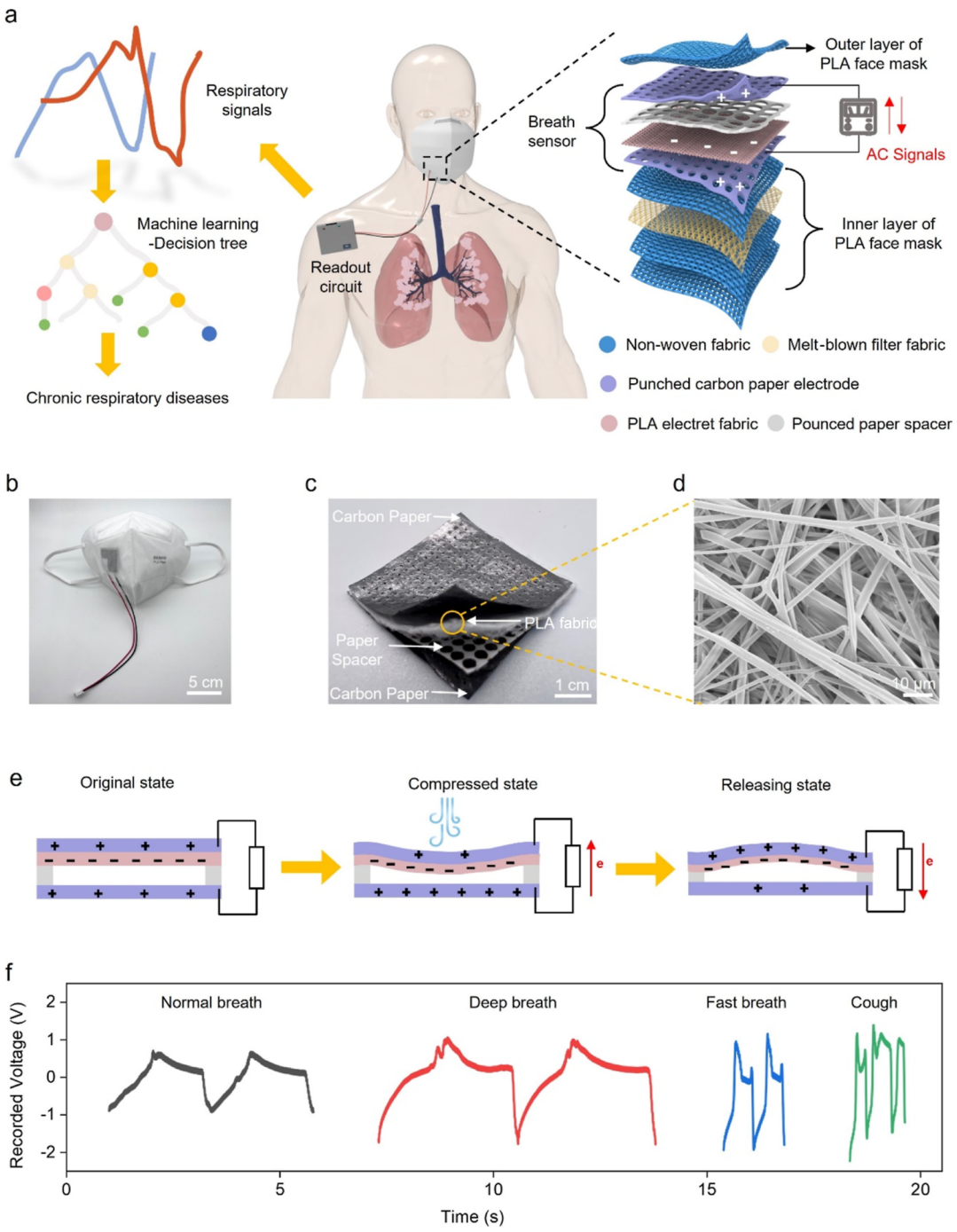

Figure 1. System design strategy. (a) Schematic illustrating the composition of a biodegradable smart face mask for diagnosing chronic respiratory diseases. The left part shows the signal processing strategy, and the right part shows the detailed structure of the breath sensor. (b) Image of a sensor assembled with a PLA-made face mask, with a pin cable for external connection. (c) Image of a sensor showing the laminated structures. (d) Surface SEM image of the PLA electret fabric. (e) Diagram illustrating the detailed working mechanism of a biodegradable self-powered breath sensor. (f) Recorded by a smart face mask, measured respiratory signals of various breathing conditions of normal breath, deep breath, fast breath, and cough.

meet the above-mentioned requirements has both clinical and practical significance.

In this work, we propose a smart face mask with a self-powered breath sensor as the sensing unit, polylactic acid (PLA)-made face mask as the main body, a portable readout circuit for signal recording, and a machine learning algorithm for chronic respiratory disease diagnosis. Our face mask can be conveniently used in daily life to collect and analyze respiratory signals without sacrificing wearing comfort. The key advancements of this work include: (1) the breath sensor can sensitively detect the respiratory waveforms of various breathing conditions, and it has been proven to work stably for 4 h in real wearable conditions; (2) the permeability resistance of the smart face mask is about 30 Pa, which is close to those of normal face masks; (3) the smart face mask is constructed with cheap and mostly biodegradable materials, the output uniformity of multiple sensors is excellent, and the readout circuit is reusable; these advantages prove its potential

https://doi.org/10.1021/acssensors.2c01628
ACS Sens. 2022, 7, 3135−3143

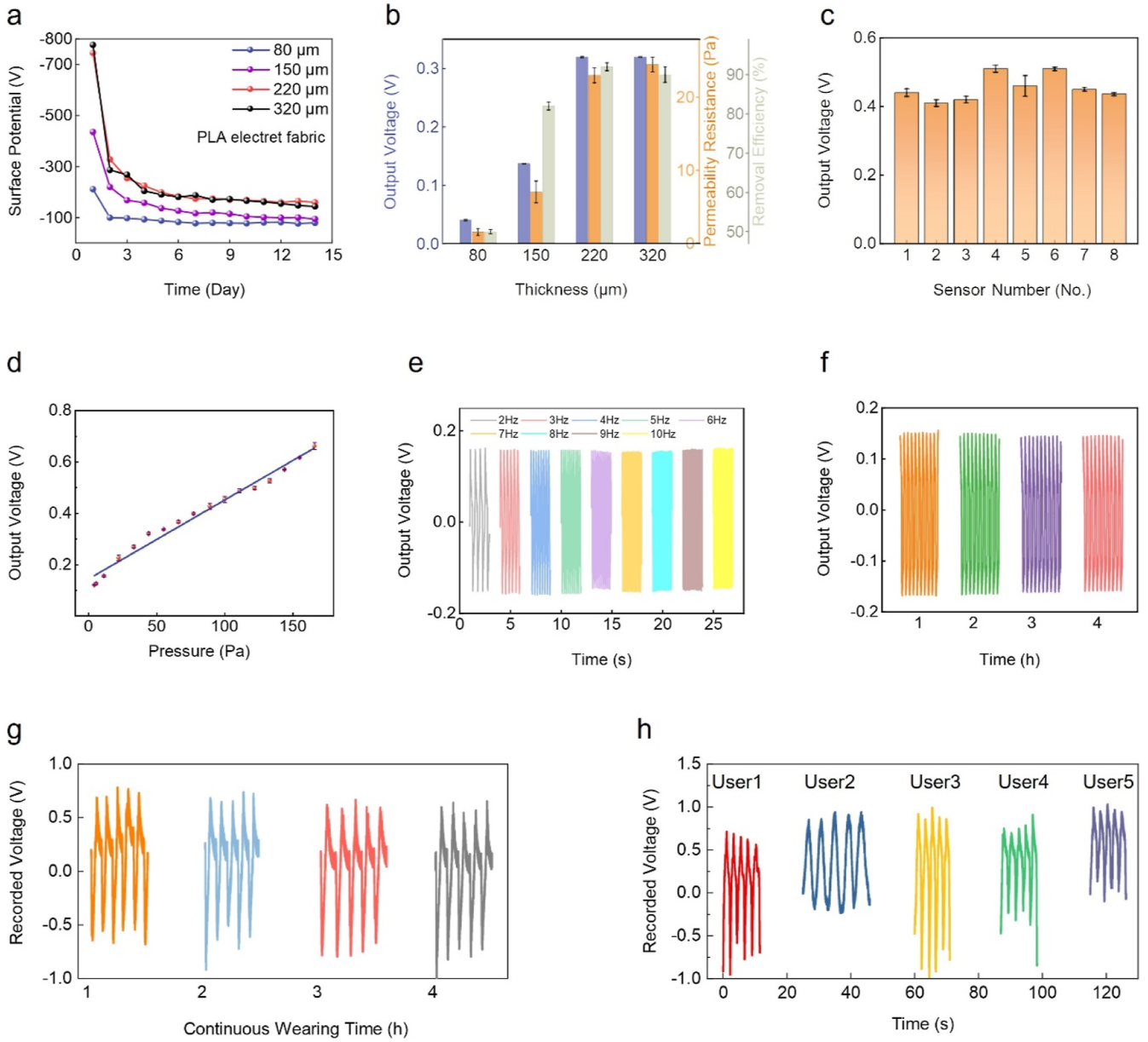

Figure 2. Performance characteristics of biodegradable self-powered breath sensors. (a) Surface potential values vs time curves for PLA electret fabrics with thicknesses of 80, 150, 220, and 320 μm. (b) Permeability resistance, removal efficiency, and peak-to-peak output voltage values of sensors based on four kinds of PLA electret fabrics; error bars mean standard deviation, and the pressure and frequency for mechanical stimulation for obtaining the outputs are 55 Pa and 5 Hz, respectively. (c) Peak-to-peak output voltage values of eight sensors, under a pressure of 100 Pa and at a frequency of 5 Hz; error bars mean standard deviation, and the sensors are randomly selected from more than 60 smart face masks fabricated in two batches. (d) Average peak-to-peak output voltage values of three sensors at a fixed frequency of 5 Hz and increasing applied pressure from 4 to 166 Pa; error bars mean standard deviation. (e) Output voltage vs time curves of a typical sensor under a fixed applied pressure of 55 Pa and various frequencies from 2 to 10 Hz. (f) Output voltage vs time curves of a typical sensor working continuously for 4 h, under an applied pressure of 55 Pa and at a frequency of 2 Hz. (g) Output voltage vs time curves recorded by a smart face mask, which is worn by a user continuously for 4 h. (h) Recorded by smart face masks, output voltage vs time curves generated by normal breathing conditions of five healthy users.

of mass usage; (4) by collaborating with a hospital to perform real case studies, we use the smart face mask to record respiratory signals of patients when they do not have obvious symptoms. A healthy group and three groups of chronic respiratory diseases (asthma, bronchitis, and COPD) are successfully classified using a bagged decision-tree algorithm with a total accuracy of up to 95.5%. This work provides a strategy to access smart face masks having great potential for practicability.

RESULTS AND DISCUSSION

System Design Strategy. The schematic of using our proposed smart face mask to diagnose chronic respiratory diseases is illustrated in Figure 1a. Specifically, a biodegradable self-powered breath sensor is assembled with a commercial PLA-made five-layer face mask to detect breathing conditions, and the outputs are recorded by a portable readout circuit that is connected to the sensor via pin cables. The detected respiratory signals are then processed with a typical bagged decision tree algorithm to diagnose respiratory diseases. The

https://doi.org/10.1021/acssensors.2c01628
ACS Sens. 2022, 7, 3135−3143

image of a PLA-made face mask assembled with a sensor is shown in Figure 1b. Using pin cables for connection means that an expensive readout circuit can be used multiple times to connect with many low-cost face masks. Figure 1c and the right part of Figure 1a indicate the image and schematic of a biodegradable self-powered breath sensor, with detailed fabrication steps shown in Figure S1 and the Methods section. Normally, the size of all sensors used in this work is 3 × 3 cm^2 and the total thickness of a sensor is about 350 μm (Figure S2). The main structure of the sensor is composed of a punched carbon paper electrode layer as the top electrode, a pounced paper spacer layer, a PLA electret fabric layer, and another punched carbon paper electrode layer as the bottom electrode. With such a design, the whole device has good air permeability. The radius of each punch hole on the two electrodes is around 0.1 mm, and the distance between the center of the circle of two holes is about 2 mm (Figure S3). The resistance of a 3 × 3 cm^2 punched carbon paper electrode is ∼5 Ω, and the conductivity under flat, 90° bending, and twisting conditions is stable, as shown in Figure S4. The PLA electret fabric is fabricated with a melt-blown method[31,32] (Figure S5) and can hold abundant electrostatic charges after polarization with the corona charging method[33] (Figure S6). The surface scanning electron microscopy (SEM) image of the PLA electret fabric in Figure 1d indicates that the diameters of the fabricated PLA fibers are normally less than 5 μm and holes with a size of tens of micrometers can ensure air permeability. The existence of the pounced paper spacer will form an air gap between the PLA electret fabric and the top electrode and avoid the electrostatic charge making contact with the top electrode to ensure the output ability of the sensor. The radius of each punch hole on the paper spacer is around 0.7 mm, and the distance between the center of the circle of two holes is about 2 mm (Figure S7). The basic working mechanism of our sensor is the electrostatic induction effect generated by the electrostatic charges on PLA electret fabric.[27,33,35] Such electrostatic charges will generate induced electrical potential on two electrodes. The dynamic breathing motions will change the air gap distance inside the sensor to cause electrical potential disequilibrium between the two electrodes. As a result, alternative electrical signals are generated in the external circuit.[36] The detailed mechanical−electrical signal conversion processes are shown in Figure 1e.[34,37]

In practical use, a breath sensor is inserted between the most outer layer and the inner layers of a PLA-made face mask so that the sensor will not affect the filtering capability of the face mask. The melt-blown filter fabric and nonwoven fabric of the face mask can also help to remove most of the moisture generated by breathing. In fact, moisture will reduce the output performances of our sensor (Figure S8). Moreover, our sensor is sensitive enough to detect the details of respiratory signals under different conditions. Various breathing conditions of normal breath, deep breath, fast breath, and cough are successfully recorded by a sensor assembled with a face mask, and the peak-to-peak output intensity of the signals measured by the portable readout circuit (with an amplifier) can reach as high as 2 to 3 V, as shown in Figure 1f. It should be noted that the intensity or waveform of each condition has a significant difference. In Figure S9, we also attach a commercial piezoelectric sensor to the chest of a volunteer to monitor respiratory signals under different conditions of normal breath, deep breath, fast breath, and cough. Actually, our respiratory sensing system is more portable and it can capture more clear details, especially for conditions of fast breath and cough.

Output Performance Characteristics. After corona charging, the surface potential values versus time curves of PLA electret fabrics with thicknesses of 80, 150, 220, and 320 μm are shown in Figure 2a, and the testing duration is 14 days. The images of these four kinds of PLA electret fabrics are shown in Figure S10. To get high surface potential, a desiccant is used in the charging chamber to lower the humidity during the corona charging process (Figure S6). The stable surface potential values of the 220 μm-thick and 320 μm-thick samples are around −160 V, which are significantly higher than those of thinner samples. To get stable performances, all the sensors we use are placed in a lab environment for more than 2 weeks (Figure S11). The permeability resistance and removal efficiency of the sensors based on four kinds of PLA electret fabrics are tested, as shown in Figure 2b. Thick samples exhibit better performances, and 220 μm-thick and 320 μm-thick samples exhibit similar performances. The permeability resistance and removal efficiency for PM 2.5 of the 220 μm-thick sample are ∼24 Pa and ∼90%, respectively. The permeability resistance is 30 to 40 Pa, and the removal efficiency is ∼90% for commercial face masks and our smart face mask (Figure S12), indicating that our sensor will not affect the basic functions of the face masks. The peak output voltage values of biodegradable self-powered breath sensors based on four kinds of PLA electret fabrics are also shown in Figure 2b. The peak-to-peak output voltage values of the 220 μm-thick sample can reach ∼0.32 V when driven by a pressure of 55 Pa and a frequency of 5 Hz. The regular mechanical stimulation is provided by a model shaker, and the electrical output testing system is shown in Figure S13. Overall, 220 μm-thick PLA electret fabrics are preferred to fabricate the sensors by considering the thickness and key performances. To verify the output uniformity of multiple sensors (Figure S14) and the potential of mass production, the peak output voltage values of eight sensors under a pressure of 100 Pa and a frequency of 5 Hz are tested and shown in Figure 2c. The peak-to-peak output voltage values are around 0.4 to 0.5 V, proving the excellent output uniformity.

Under a fixed frequency of 5 Hz and a pressure from 4 to 166 Pa, the average peak-to-peak output voltage values of the three sensors are shown in Figure 2d. In fact, the air pressure generated by breathing motions is normally below 150 Pa.[7,36] The output values have an approximately linear increase with increasing pressure applied to the sensor, from 0.12 V at 4 Pa to 0.64 V at 166 Pa. The peak output voltage of our sensor is lower than previously reported ultrathin electret-based breath sensors (5.5 μm/4.5 mg)[6] as the weight of our sensor (0.2−0.3 g) is higher and the charge density of the degradable PLA electret is lower than the nondegradable Teflon AF electret. On the other hand, Figure 2e shows the output voltage versus time curves of a typical sensor under a fixed applied pressure of 55 Pa and a frequency from 2 to 10 Hz. The corresponding peak-to-peak output voltage values remain stable at around 0.3 V for various testing frequencies. The peak-to-peak output voltage of our sensor is mainly affected by the applied pressure, while the peak output current is affected by the pressure and frequency (Figure S15), meaning that our sensor has similar output characteristics to other electrostatic-based sensors. To test the output stability, mechanical stimulation with a pressure of 55 Pa and a frequency of 2 Hz is applied on a typical sensor for a continuous 4 h, as shown in Figure 2f. During the 28,800

https://doi.org/10.1021/acssensors.2c01628
ACS Sens. 2022, 7, 3135−3143

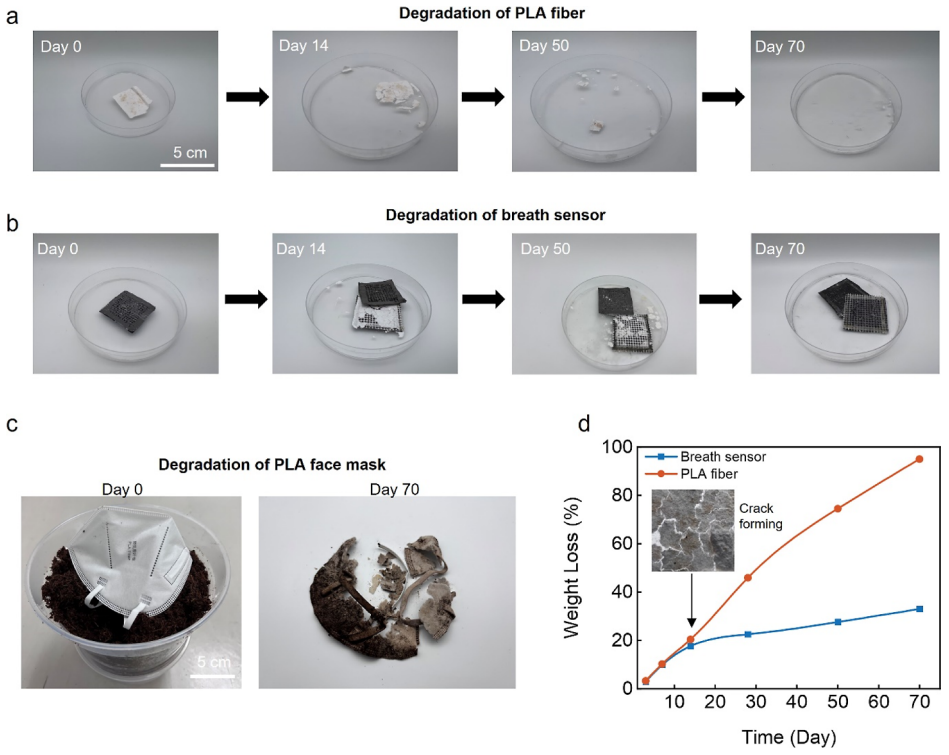

Figure 3. Biodegradable performances. (a) Images of the PLA electret fabric at various stages of biodegradation. (b) Images of the biodegradable self-powered breath sensor at various stages of biodegradation. (c) Images of the commercial PLA-made mask biodegradation on day 0 and day 70. (d) Weight loss trends of the PLA electret fabric and the sensor; the insert shows cracks formed in the PLA electret fabric. Machine learning-assisted chronic respiratory disease diagnosis.

testing cycles, the corresponding peak-to-peak output voltage values remain stable at around 0.30 to 0.32 V, indicating the excellent output stability of our sensor, which is a critical parameter ensuring practicability.

The output stability of a biodegradable self-powered breath sensor assembled into a smart face mask is also tested, which is worn by a user continuously for 4 h, as shown in Figure 2g. It is proven that our sensor retains excellent output stability in real wearing conditions. It is suggested by medical doctors that a user should replace a face mask every 4 h. Furthermore, the respiratory signals generated by normal breathing conditions of five healthy users are measured and shown in Figure 2h. The typical breathing features of each user are successfully recorded to further prove the good reliability of our sensor.

Biodegradable Performances. Most of the traditional face masks are made of polypropylene,[38,39] which is sourced from fossil fuels, and are nonbiodegradable. This fact indicates that these face masks will not decompose and exist for a tremendously long time in the natural environment. In our smart face masks, the main body is fabricated with biodegradable PLA; the functional component of the biodegradable self-powered breath sensor is based on PLA, cellulose-based paper, and a carbon electrode; the portable readout circuit is reusable. Therefore, it will not cause serious pollution problems during mass usage. The hydrolytic and microbial degradation mechanisms play a significant role in PLA degradation.[38] Based on these mechanisms, PLA electret fabric pieces and sensors are placed in Petri dishes with pure water and microorganisms (Figure S16) so that we can easily observe the whole degradation process and measure the weight loss versus time curves. Then, these Petri dishes are placed in a thermotank kept at 60° to accelerate hydrolysis. At the same time, a commercial PLA-made mask is buried in the soil of a pot to mimic natural degradation. Similarly, the pot is also placed in the thermotank. The pot and Petri dishes are filled with water daily to ensure a high-humidity environment. The ester groups of the main chain of PLA are cleaved in the degradation process, and the weight of PLA decreases.[40−42] The images of the degradation process of the PLA electret fabric are shown in Figure 3a. On day 14 of the PLA degradation process, the main structure of PLA electret fabric begins to crumble and the degradation almost finishes by day 70. The images of the degradation process of the sensor in Figure 3b show that the degradation of paper-based components is not very good on day 70, whereas the PLA electret fabric in the sensor has nearly biodegraded. In fact, paper-based components also begin to degrade, but they need a longer time to be fully biodegraded. For the degradation process of the PLA-made face mask, less than 15% of the face mask remains on day 70, as shown in Figure 3c, demonstrating that even in soil, microbes and water can quickly decompose the face mask. Figure 3d shows the weight loss trends of the PLA electret fabric and the sensor, and it is found that the PLA electret fabric degrades more quickly after forming cracks on day 14. On day 70, the degradation rate of the PLA electret fabric and the sensor is 33 and 95%, respectively.

Collaborating with a hospital in Zhuhai, China, to perform a real case study, we use smart face masks to diagnose three typical chronic respiratory diseases such as asthma, bronchitis, and COPD. Figure 4a shows the respiratory signal recording process for a user, and the enlarged image shows the detail of the portable readout circuit. The readout circuit is attached to the main body of the volunteer; normally it does not need any special treatment, such as disinfection. Here, the green LED is

https://doi.org/10.1021/acssensors.2c01628
ACS Sens. 2022, 7, 3135−3143

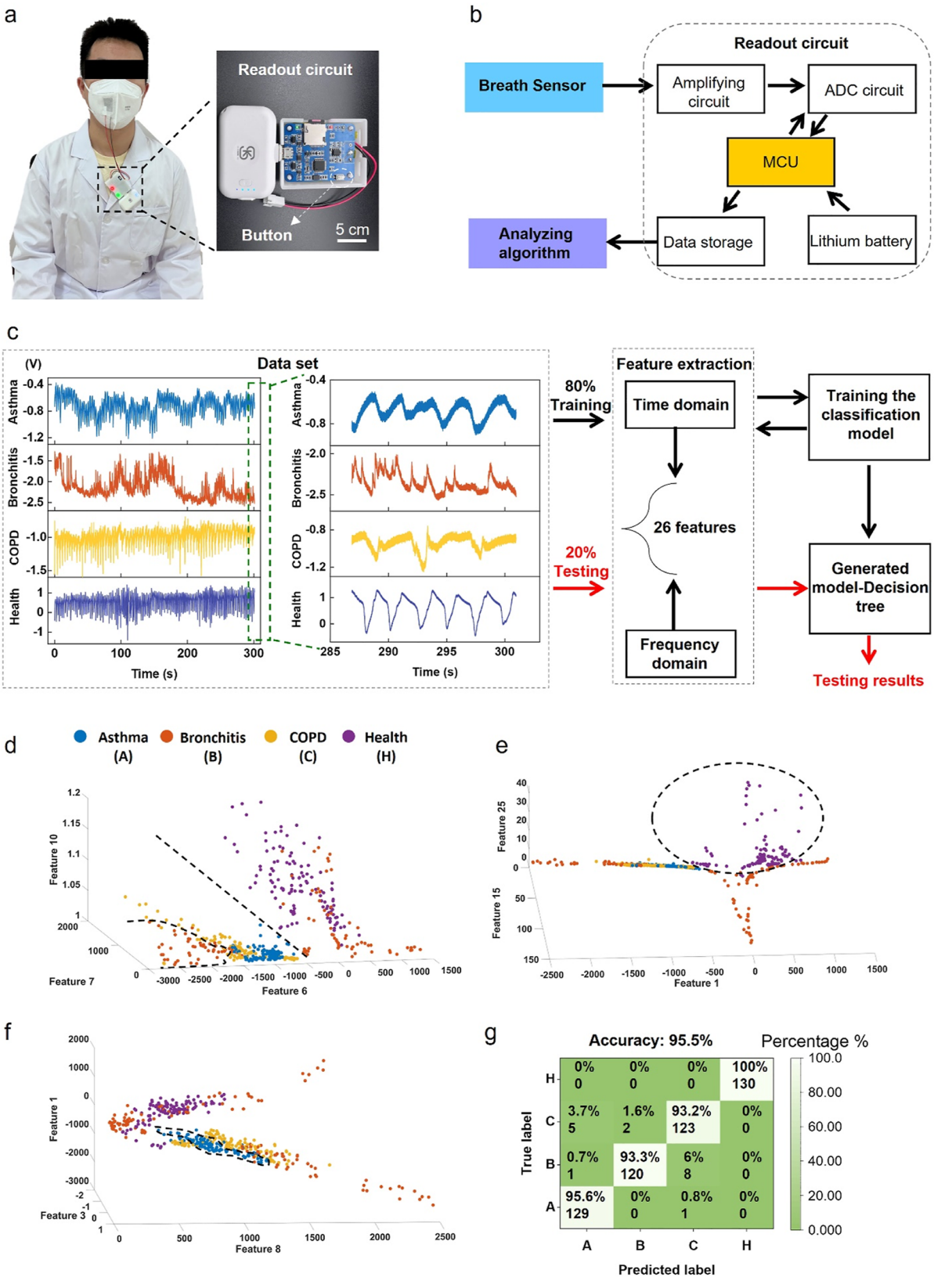

Figure 4. Chronic respiratory disease diagnosis by the smart face mask. (a) Image illustrating the respiratory signal recording process, and the enlarged image shows the portable readout circuit. (b) Flowchart of the respiratory signal recording process. (c) Left part: typical recorded respiratory signals and their enlarged view from healthy volunteers and patients with asthma, bronchitis, and COPD. Right part: flowchart of the machine learning process. (d) 3D scatter plot with feature 6, feature 7, and feature 10 as the coordinate axes to divide healthy and bronchitis as one group and asthma and COPD as another group. (e) 3D scatter plot with feature 1, feature 15, and feature 25 as coordinate axes to divide healthy and bronchitis groups. (f) 3D scatter plot with feature 1, feature 3, and feature 8 as coordinate axes to divide asthma and COPD groups. (g) Confusion matrix showing the classification results of healthy (H) group, COPD (C) group, bronchitis (B) group, and asthma (A) group.

https://doi.org/10.1021/acssensors.2c01628
ACS Sens. 2022, 7, 3135−3143

a power indicator, and the red LED is a status indicator triggered by a white button for indicating the signal recording process. The detailed workflow is shown in Figure 4b. Specifically, the respiratory signals are measured using a breath sensor and then amplified by three times using an amplifying circuit; the amplified analog signals are converted into digital signals by an analog-to-digital converter circuit; the digital signals are processed by a multicontroller unit (MCU) and then stored in a data storage component (micro-SD), and finally, the recorded respiratory signals are classified using a typical machine learning algorithm. The detailed design for the readout circuit is shown in Figure S17. The data recording rate and time are 500 points/s and 5 min. Wireless communication devices with low power and small size can only transmit a low sampling rate of about 50 points/s. To more accurately diagnose chronic respiratory diseases in a real case study, more details of respiratory signals should be captured. Our system can record a high sampling rate of 500 points/s, which obtains better waveforms for machine learning. The readout circuit is powered by a small lithium battery with a capacity of 1200 mAh, and this battery can support the system for up to 16.5 h (Figure S18). The total weight of the sensor, the face mask, and the readout circuit is about 60 g.

It should be noted that the respiratory signals of patients are recorded when they are in normal states and have no obvious symptoms. The respiratory signals of five healthy volunteers, six patients with asthma, four patients with bronchitis, and five patients with COPD are recorded and analyzed in this work. Figure S19 shows the signal recording process of patients in the hospital, and Figure S20 provides basic information about the volunteers, such as gender, age, and smoking habits. All volunteers are tested in a static sitting condition and indoors. Normally, it takes less than 1 day to finish respiratory signal collection and classification processes. Typical recorded respiratory signals and their enlarged view of healthy volunteers and patients are shown in the left part of Figure 4c. The decision tree algorithm is used for the classification of signals, and we use a bagged ensemble strategy in the decision tree to achieve high accuracy of classification,[43,44] with the specific parameters shown in Table S1. The flow chart of the machine learning process is shown in the right part of Figure 4c. A complete breathing waveform is defined as a data set, and 2400 data sets in total are obtained. We extract 26 typical features based on the time domain and frequency domain for each data set, with the details of all features given in Table S2. The definition of the main factors is given in Table S3. Among all the data sets, we randomly extract 80% as the training set and validate the remaining 20% after the model has been trained.

The asthma, bronchitis, COPD, and health groups are successfully classified by our bagged decision tree model. To intuitively show the classification ability, 3D scatter plots are provided to show the classification results of test data sets. Typically, Figure 4d shows a 3D scatter plot with feature 6, feature 7, and feature 10 as coordinate axes, in which the data sets are clearly divided into two groups as marked by the dashed lines: healthy and bronchitis in one group and asthma and COPD in another group. In Figure 4e, with feature 1, feature 15, and feature 25 as coordinate axes, healthy and bronchitis groups are divided. Furthermore, in Figure 4f, with feature 1, feature 3, and feature 8 as coordinate axes, asthma and COPD groups are also divided. In fact, the total classification accuracy is contributed by all 26 typical features. As shown in the confusion matrix in Figure 4g, the total classification accuracy for distinguishing healthy and disease groups is up to 95.5%, with an accuracy of 100% for the healthy group, an accuracy of 93.2% for the COPD group, an accuracy of 93.3% for the bronchitis group, and an accuracy of 95.6% for the asthma group, respectively. These results indicate that healthy people can be easily distinguished and typical chronic respiratory diseases can be effectively diagnosed by our method.

CONCLUSIONS

In summary, we develop a biodegradable self-powered breath sensor with excellent air permeability based on a PLA electric fabric, pounced carbon paper electrodes, and a pounced paper spacer, and the sensor is integrated with a PLA-made face mask and a portable readout circuit to form a smart face mask. The output sensitivity, stability, and uniformity of the smart face mask are proven to be good in real wearable conditions. The smart face mask is eco-friendly and has the potential for mass production. As a typical demonstration, smart face masks are successfully used to diagnose three typical chronic respiratory diseases of asthma, bronchitis, and COPD, with the machine learning algorithm of the bagged decision-tree model as a data analysis mean. The total accuracy for distinguishing the healthy group and the three chronic respiratory disease groups is up to 95.5%. Future works to further improve the performances of our smart face mask include but are not limited to (1) ensuring the output performances of the sensor under harsh environments, (2) lowering the weight of the readout circuit to improve the portability, and (3) recording and analyzing the respiratory signals in real time.

METHODS

Fabrication of the PLA Electret Fabric. The PLA electret powders were bought from Natureworks LLC (Ingeo 6252D). The PLA electret fabric was fabricated via the melt-blown method. First, PLA powders were melted in a hot barrel at a temperature of 220 °C, and then the melted PLA was extruded through a spinning die under a melt-blown pressure of 0.2 MPa. At the same time, hot air with a temperature of 220 °C and a pressure of 0.2 MPa was applied to the spinning die to make the molten PLA into fabric shape. A collector with rotating and reciprocating motion was placed 14 cm below the spinning die to collect the PLA electret fabric. The reciprocating motion speed was 1 mm/s, with a displacement of 30 cm. The rotating motion speed was 6 rpm. The thickness of the PLA electret fabric was controlled by the collection time, which were 20, 30, and 40 min for 150, 220, and 320 μm, respectively. For the 80 μm-thick sample, the hot air temperature was decreased to 190 °C with other parameters retained, and the collection time was 20 min.

Fabrication of the Biodegradable Self-Powered Breath Sensor. The detailed fabrication steps are shown in Figure S1. Step I—punch holes: a laser (Mingchuang 4060, 70 W) is used to punch a circular hole on conductive carbon paper with a carbon layer of 20 μm, a paper layer of 100 μm, and a size of 3 × 3 cm^2. The radius of each punch hole is set as 0.1 mm, and the distance between the center of the circle of two holes is set as 2 mm. Step II—adhere it to the electret: a PLA electret fabric with a size of 3 × 3 cm^2 is pasted on the carbon paper electrode with double-sided tape fixing the four boundaries. Step III—corona charging: the corona charging method is used to generate negative electrostatic charges on the PLA electret fabric. In specific, as shown in Figure S5, the PLA surface not pasted on the carbon paper faces the corona needle tip at a distance of 5 cm. The charging voltage generated by a high voltage source (Dongwen DW-N503-4ACD2) is −16 kV. The charging time is 5 min. Step IV—punch holes: a laser (Snapmaker A350T, 1.6 W) is used to punch a circular hole on an A4 paper to form the punched paper spacer. The

https://doi.org/10.1021/acssensors.2c01628
ACS Sens. 2022, 7, 3135−3143

radius of each punch hole is set as 0.7 mm, and the distance between the center of the circle of two holes is set as 2 mm. Step V—adhere it to the spacer: a punched paper spacer with a size of 3 × 3 cm^2 is covered on the charged PLA surface with four boundaries fixed with a double-sided tape. Step VI—adhere it to the top electrode: Another carbon electrode with a size of 3 × 3 cm^2 is covered on the spacer with four boundaries fixed with double-sided tape.

Fabrication of the Biodegradable Smart Face Mask. The main body of the biodegradable smart face mask is a commercial PLA-made five-layer face mask bought from Health Box. A biodegradable self-powered breath sensor is inserted between the most outer layer and other layers of the PLA face mask to form the biodegradable smart face mask. The sensor is connected to an external readout circuit via pin cables.

Material and Device Characterization. The SEM images are measured by high-resolution field emission SEM (Sigma FE-SEM, Zeiss Corporation, Germany). The surface potential of the samples is tested using an electrostatic voltmeter (Trek 347). The conductivity of the samples is measured using a Keithley 2400 source meter. The outputs of the samples are measured by a self-made portable readout circuit or an electromechanical output testing system. In this system, the outputs are measured by a NI USB 6341 data acquisition system, and regular mechanical stimulation applied to the samples is provided by a modal shaker (JZK-10, Sinocera Piezotronics, Inc. China) controlled by a YE1311 (Sinocera Piezotronics, China) sweep signal generator and a YE5872A (Sinocera Piezotronics, China) power amplifier. The study protocol is thoroughly reviewed and approved by the ethical committee of the University of Macau (approval number BSERE21-APP022-FST). Informed signed consent for the volunteer tests has been obtained from the volunteers prior to their participation in this study.

■ ASSOCIATED CONTENT

Supporting Information

The Supporting Information is available free of charge at https://pubs.acs.org/doi/10.1021/acssensors.2c01628.

Fabrication process and relative characteristics of the biodegradable self-powered breath sensor and smart face mask, relative information about the machine learning process, design of the readout circuit, and additional description (PDF)

■ AUTHOR INFORMATION

Corresponding Author

Junwen Zhong − *Department of Electromechanical Engineering and Centre for Artificial Intelligence and Robotics, University of Macau, Macau SAR 999078, China;* orcid.org/0000-0002-0232-1604; Email: junwenzhong@um.edu.mo

Authors

Kaijun Zhang − *Department of Electromechanical Engineering and Centre for Artificial Intelligence and Robotics, University of Macau, Macau SAR 999078, China;* orcid.org/0000-0002-9924-2928

Zhaoyang Li − *Department of Electromechanical Engineering and Centre for Artificial Intelligence and Robotics, University of Macau, Macau SAR 999078, China*

Jianfeng Zhang − *Department of Electromechanical Engineering and Centre for Artificial Intelligence and Robotics, University of Macau, Macau SAR 999078, China; Laboratory of Electret & Its Application, Hangzhou Dianzi University, Hangzhou 310018, China*

Dazhe Zhao − *Department of Electromechanical Engineering and Centre for Artificial Intelligence and Robotics, University of Macau, Macau SAR 999078, China*

Yucong Pi − *Department of Electromechanical Engineering and Centre for Artificial Intelligence and Robotics, University of Macau, Macau SAR 999078, China*

Yujun Shi − *Department of Electromechanical Engineering and Centre for Artificial Intelligence and Robotics, University of Macau, Macau SAR 999078, China*

Renkun Wang − *Department of Electromechanical Engineering and Centre for Artificial Intelligence and Robotics, University of Macau, Macau SAR 999078, China*

Peisheng Chen − *Zhuhai Hospital of Integrated Traditional Chinese & Western Medicine, Zhuhai 519000, China*

Chaojie Li − *Zhuhai Hospital of Integrated Traditional Chinese & Western Medicine, Zhuhai 519000, China*

Gangjin Chen − *Laboratory of Electret & Its Application, Hangzhou Dianzi University, Hangzhou 310018, China;* orcid.org/0000-0001-6022-1700

Iek Man Lei − *Department of Electromechanical Engineering and Centre for Artificial Intelligence and Robotics, University of Macau, Macau SAR 999078, China*

Complete contact information is available at: https://pubs.acs.org/10.1021/acssensors.2c01628

Author Contributions

¶K.Z. and Z.L contributed equally to this work.

Notes

The authors declare no competing financial interest.

■ ACKNOWLEDGMENTS

We acknowledge the funding support from the Science and Technology Development Fund, Macau SAR (FDCT) (file no. 0059/2021/AFJ, 0040/2021/A1), Start Research Grant from the University of Macau (SRG2021-00001-FST), and Multi-Year Research Grant (MYRG2022-00003-FST).

■ REFERENCES

(1) Brooks, J. T.; Butler, J. C. Effectiveness of Mask Wearing to Control Community Spread of SARS-CoV-2. *J. Am. Med. Assoc.* **2021**, *325*, 998−999.

(2) Cheng, K. K.; Lam, T. H.; Leung, C. C. Wearing Face Masks in the Community during the COVID-19 Pandemic: Altruism and Solidarity. *Lancet* **2022**, *399*, e39−e40.

(3) Tabatabaeizadeh, S. A. Airborne Transmission of COVID-19 and the Role of Face Mask to Prevent It: A Systematic Review and Meta-Analysis. *Eur. J. Med. Res.* **2021**, *26*, 1−6.

(4) Kissler, S. M.; Tedijanto, C.; Goldstein, E.; Grad, Y. H.; Lipsitch, M. Projecting the Transmission Dynamics of SARS-CoV-2 through the Postpandemic Period. *Science* **2020**, *368*, 860−868.

(5) Techasatian, L.; Lebsing, S.; Uppala, R.; Thaowandee, W.; Chaiyarit, J.; Supakunpinyo, C.; Panombualert, S.; Mairiang, D.; Saengnipanthkul, S.; Wichajarn, K.; Kiatchoosakun, P.; Kosalaraksa, P. The Effects of the Face Mask on the Skin Underneath: A Prospective Survey During the COVID-19 Pandemic. *J. Prim. Care Community Health* **2020**, *11*, 2150132720966167.

(6) Zhong, J.; Li, Z.; Takakuwa, M.; Inoue, D.; Hashizume, D.; Jiang, Z.; Shi, Y.; Ou, L.; Nayeem, M. O. G.; Umezu, S.; Fukuda, K.; Someya, T. Smart Face Mask Based on an Ultrathin Pressure Sensor for Wireless Monitoring of Breath Conditions. *Adv. Mater.* **2022**, *34*, 2107758.

(7) Escobedo, P.; Fernández-Ramos, M. D.; López-Ruiz, N.; Moyano-Rodríguez, O.; Martínez-Olmos, A.; Pérez de Vargas-Sansalvador, I. M.; Carvajal, M. A.; Capitán-Vallvey, L. F.; Palma, A. J. Smart facemask for wireless CO2 monitoring. *Nat. Commun.* **2022**, *13*, 72.

(8) Ferkol, T.; Schraufnagel, D. The Global Burden of Respiratory Disease. *Ann. Am. Thorac. Soc.* **2014**, *11*, 404−406.

(9) Gibson, G. J.; Loddenkemper, R.; Lundbäck, B.; Sibille, Y. Respiratory Health and Disease in Europe: The New European Lung White Book. *Eur. Respir. J.* **2013**, *42*, 559−563.
(10) Pan, L.; Wang, C.; Jin, H.; Li, J.; Yang, L.; Zheng, Y.; Wen, Y.; Tan, B. H.; Loh, X. J.; Chen, X. Lab-on-Mask for Remote Respiratory Monitoring. *ACS Mater. Lett.* **2020**, *2*, 1178−1181.
(11) Ye, Z.; Ling, Y.; Yang, M.; Xu, Y.; Zhu, L.; Yan, Z.; Chen, P.-Y. A Breathable, Reusable, and Zero-Power Smart Face Mask for Wireless Cough and Mask-Wearing Monitoring. *ACS Nano* **2022**, *16*, 5874−5884.
(12) Liu, Y.; Zhao, L.; Avila, R.; Yiu, C.; Wong, T.; Chan, Y.; Yao, K.; Li, D.; Zhang, Y.; Li, W.; Xie, Z.; Yu, X. Epidermal Electronics for Respiration Monitoring via Thermo-Sensitive Measuring. *Mater. Today Phys.* **2020**, *13*, 100199.
(13) Pang, Y.; Jian, J.; Tu, T.; Yang, Z.; Ling, J.; Li, Y.; Wang, X.; Qiao, Y.; Tian, H.; Yang, Y.; Ren, T.-L. Wearable Humidity Sensor Based on Porous Graphene Network for Respiration Monitoring. *Biosens. Bioelectron.* **2018**, *116*, 123−129.
(14) Li, B.; Xiao, G.; Liu, F.; Qiao, Y.; Li, C.; Lu, Z. A Flexible Humidity Sensor Based on Silk Fabrics for Human Respiration Monitoring. *J. Mater. Chem. C* **2018**, *6*, 4549−4554.
(15) Duan, Z.; Jiang, Y.; Yan, M.; Wang, S.; Yuan, Z.; Zhao, Q.; Sun, P.; Xie, G.; Du, X.; Tai, H. Facile, Flexible, Cost-Saving, and Environment-Friendly Paper-Based Humidity Sensor for Multifunctional Applications. *ACS Appl. Mater. Interfaces* **2019**, *11*, 21840−21849.
(16) Ma, L.; Wu, R.; Patil, A.; Zhu, S.; Meng, Z.; Meng, H.; Hou, C.; Zhang, Y.; Liu, Q.; Yu, R.; Wang, J.; Lin, N.; Liu, X. Y. Full-Textile Wireless Flexible Humidity Sensor for Human Physiological Monitoring. *Adv. Funct. Mater.* **2019**, *29*, 1904549.
(17) Duan, Z.; Jiang, Y.; Tai, H. Recent Advances in Humidity Sensors for Human Body Related Humidity Detection. *J. Mater. Chem. C* **2021**, *9*, 14963−14980.
(18) Ghosh, R.; Song, M. S.; Park, J.; Tchoe, Y.; Guha, P.; Lee, W.; Lim, Y.; Kim, B.; Kim, S.-W.; Kim, M.; Yi, G.-C. Fabrication of Piezoresistive Si Nanorod-Based Pressure Sensor Arrays: A Promising Candidate for Portable Breath Monitoring Devices. *Nano Energy* **2021**, *80*, 105537.
(19) Massaroni, C.; Di Tocco, J.; Lo Presti, D.; Longo, U. G.; Miccinilli, S.; Sterzi, S.; Formica, D.; Saccomandi, P.; Schena, E. Smart Textile Based on Piezoresistive Sensing Elements for Respiratory Monitoring. *IEEE Sens. J.* **2019**, *19*, 7718−7725.
(20) Park, S. W.; Das, P. S.; Chhetry, A.; Park, J. Y. A Flexible Capacitive Pressure Sensor for Wearable Respiration Monitoring System. *IEEE Sens. J.* **2017**, *17*, 6558−6564.
(21) Min, S. D.; Yun, Y.; Shin, H. Simplified Structural Textile Respiration Sensor Based on Capacitive Pressure Sensing Method. *IEEE Sens. J.* **2014**, *14*, 3245−3251.
(22) Liu, Z.; Zhang, S.; Jin, Y. M.; Ouyang, H.; Zou, Y.; Wang, X. X.; Xie, L. X.; Li, Z. Flexible Piezoelectric Nanogenerator in Wearable Self-Powered Active Sensor for Respiration and Healthcare Monitoring. *Semicond. Sci. Technol.* **2017**, *32*, 064004.
(23) Maity, K.; Garain, S.; Henkel, K.; Schmeißer, D.; Mandal, D. Self-Powered Human-Health Monitoring through Aligned PVDF Nanofibers Interfaced Skin-Interactive Piezoelectric Sensor. *ACS Appl. Polym. Mater.* **2020**, *2*, 862−878.
(24) Ning, C.; Cheng, R.; Jiang, Y.; Sheng, F.; Yi, J.; Shen, S.; Zhang, Y.; Peng, X.; Dong, K.; Wang, Z. L. Helical Fiber Strain Sensors Based on Triboelectric Nanogenerators for Self-Powered Human Respiratory Monitoring. *ACS Nano* **2022**, *16*, 2811−2821.
(25) Zhao, Z.; Yan, C.; Liu, Z.; Fu, X.; Peng, L.-M.; Hu, Y.; Zheng, Z. Machine-Washable Textile Triboelectric Nanogenerators for Effective Human Respiratory Monitoring through Loom Weaving of Metallic Yarns. *Adv. Mater.* **2016**, *28*, 10267−10274.
(26) Shen, S.; Xiao, X.; Xiao, X.; Chen, J. Triboelectric Nanogenerators for Self-Powered Breath Monitoring. *ACS Appl. Energy Mater.* **2022**, *5*, 3952−3965.
(27) Lin, S.; Wang, S.; Yang, W.; Chen, S.; Xu, Z.; Mo, X.; Zhou, H.; Duan, J.; Hu, B.; Huang, L. Trap-Induced Dense Monocharged Perfluorinated Electret Nanofibers for Recyclable Multifunctional Healthcare Mask. *ACS Nano* **2021**, *15*, 5486−5494.
(28) Cheng, Y.; Wang, C.; Zhong, J.; Lin, S.; Xiao, Y.; Zhong, Q.; Jiang, H.; Wu, N.; Li, W.; Chen, S.; Wang, B.; Zhang, Y.; Zhou, J. Electrospun Polyetherimide Electret Nonwoven for Bi-Functional Smart Face Mask. *Nano Energy* **2017**, *34*, 562−569.
(29) Dinh, T.; Nguyen, T.; Phan, H.-P.; Nguyen, N.-T.; Dao, D. V.; Bell, J. Stretchable Respiration Sensors: Advanced Designs and Multifunctional Platforms for Wearable Physiological Monitoring. *Biosens. Bioelectron.* **2020**, *166*, 112460.
(30) Bokka, N.; Karhade, J.; Sahatiya, P. Deep Learning Enabled Classification of Real-Time Respiration Signals Acquired by MoSSe Quantum Dot-Based Flexible Sensors. *J. Mater. Chem. B* **2021**, *9*, 6870−6880.
(31) Chen, G.; Zhang, J.; Shi, X.; Peng, H.; Chen, X. Charge Trapped Mechanism for Semi-Crystalline Polymer Electrets: Quasi-Dipole Model. *IET Nanodielectr.* **2020**, *3*, 81−87.
(32) Zhang, J.; Chen, G.; Bhat, G. S.; Azari, H.; Pen, H. Electret Characteristics of Melt-Blown Polylactic Acid Fabrics for Air Filtration Application. *J. Appl. Polym. Sci.* **2020**, *137*, 48309.
(33) Leal Ferreira, G. F.; Figueiredo, M. T. Corona Charging of Electrets: Models and Results. *IEEE Trans. Electr. Insul.* **1992**, *27*, 719−738.
(34) Fan, F. R.; Tang, W.; Wang, Z. L. Flexible Nanogenerators for Energy Harvesting and Self-Powered Electronics. *Adv. Mater.* **2016**, *28*, 4283−4305.
(35) Zhong, J.; Ma, Y.; Song, Y.; Zhong, Q.; Chu, Y.; Karakurt, I.; Bogy, D. B.; Lin, L. A Flexible Piezoelectret Actuator/Sensor Patch for Mechanical Human-Machine Interfaces. *ACS Nano* **2019**, *13*, 7107−7116.
(36) Li, W.; Wu, N.; Zhong, J.; Zhong, Q.; Zhao, S.; Wang, B.; Cheng, X.; Li, S.; Liu, K.; Hu, B.; Zhou, J. Theoretical Study of Cellular Piezoelectret Generators. *Adv. Funct. Mater.* **2016**, *26*, 1964−1974.
(37) Mhetre, M. R.; Abhyankar, H. K. Human Exhaled Air Energy Harvesting with Specific Reference to PVDF Film. *Eng. Sci. Technol.* **2017**, *20*, 332−339.
(38) Fadare, O. O.; Okoffo, E. D. Covid-19 Face Masks: A Potential Source of Microplastic Fibers in the Environment. *Sci. Total Environ.* **2020**, *737*, 140279.
(39) Dharmaraj, S.; Ashokkumar, V.; Hariharan, S.; Manibharathi, A.; Show, P. L.; Chong, C. T.; Ngamcharussrivichai, C. The COVID-19 Pandemic Face Mask Waste: A Blooming Threat to the Marine Environment. *Chemosphere* **2021**, *272*, 129601.
(40) Zaaba, N. F.; Jaafar, M. A Review on Degradation Mechanisms of Polylactic Acid: Hydrolytic, Photodegradative, Microbial, and Enzymatic Degradation. *Polym. Eng. Sci.* **2020**, *60*, 2061−2075.
(41) Farah, S.; Anderson, D. G.; Langer, R. Physical and Mechanical Properties of PLA, and Their Functions in Widespread Applications—A Comprehensive Review. *Adv. Drug Deliver Rev.* **2016**, *107*, 367−392.
(42) Elsawy, M. A.; Kim, K.-H.; Park, J.-W.; Deep, A. Hydrolytic Degradation of Polylactic Acid (PLA) and Its Composites. *Renewable Sustainable Energy Rev.* **2017**, *79*, 1346−1352.
(43) Krzywinski, M.; Altman, N. Classification, and regression trees. *Nat. Methods* **2017**, *14*, 757−758.
(44) Askari, H.; Xu, N.; Groenner Barbosa, B. H.; Huang, Y.; Chen, L.; Khajepour, A.; Chen, H.; Wang, Z. L. Intelligent Systems Using Triboelectric, Piezoelectric, and Pyroelectric Nanogenerators. *Mater. Today* **2022**, *52*, 188−206.

https://doi.org/10.1021/acssensors.2c01628
ACS Sens. 2022, 7, 3135−3143